NAIC-ID(RS)T-0369-94

NATIONAL AIR INTELLIGENCE CENTER

SIGNALS PROCESSING USING ACOUSTO-OPTICAL TECHNOLOGY

by

Li Ning

NAIC-ID(RS)T-0369-94

HUMAN TRANSLATION

NAIC-ID(RS)T-0369-94 14 November 1994

MICROFICHE NR: 94C000474L

SIGNALS PROCESSING USING ACOUSTO-OPTICAL TECHNOLOGY

By: Li Ning

English pages: 10

Source: Guangxue Xuebao, Vol 8, Nr. 5, May 1988; pp. 429-434

Country of origin: China
Translated by: Leo Kanner Associates
F33657-88-D-2188
Quality Control: Nancy L. Burns
Requester: NAIC/TATA/J.M. Finley

GRAPHICS DISCLAIMER

All figures, graphics, tables, equations, etc. merged into this translation were extracted from the best quality copy available.

SIGNAL PROCESSING USING ACOUSTO-OPTICAL TECHNOLOGY

LI NING

Department of Engineering Mechanics, Chengdu University of Science and Technology.

Received 3 April 1987, revised 15 May, 1987

An experimental system for simulative signals processing using high frequency wideband acousto-optical device is proposed herein and the mathematical expressions of system output are derived. The experimental results of both space and time integrating convolution (correlation) for the simulative signals composed of root impulses conform on the whole with calculations.

I: INTRODUCTION: In current signals processing technology, various types of super fast instantaneous wideband complex signals often occur, and the use of electronic signals processing encounters a number of difficulties. However, there are a number of special advantages to using optical signals processing technology to process these complex signals. After the mid seventies, the theory and manufacturing technology for acousto-optical signals processing technology continued to be improved, making possible live time optical signals processing. Acousto-optical signals processing technology is not only appropriate for radar signals, sonar signals and communications signals, but it is also appropriate for various wide band high speed signals. It uses non sweep methods of parallel processing of multiple channel signals. It has 100 percent intercept rate. It can also perform live time processing. Research has demonstrated that it can be used to manufacture various types of special use acousto-optical signals processing equipment[1]. Demetri Psaltis systematically summarized the mathematical formulas for the output of the various processors[2]. For our own experiments, we manufactured high

frequency wide band acousto-optical devices of our own design to increase the system band width. Be appropriately adjusting the equipment in our experiments, it was possible to set up structures for both space and time integrated signals. It was also possible to use both direct and heterodyne detection.

II: MATHEMATICAL MODEL OF ACOUSTO-OPTICAL SIGNALS PROCESSOR

There are two basic models for acousto-optical signals processors, the spacial integration model where a lens effects the integration and the time integration model where a detector effects the integration.

1. THE SPACE INTEGRATION MODEL

FIGURE 1: SPACE INTEGRATING A-O CORRELATION

FIGURE 2: SPACE INTEGRATING A-O CORRELATION USING HETERODYNE DETECTOR

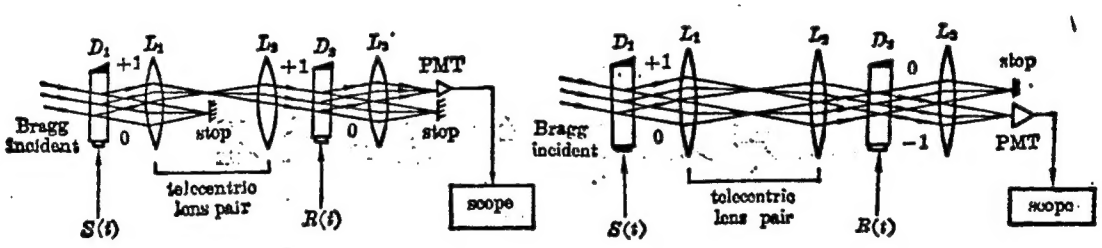

A Spacial integration model acousto-optical correlation (convoluting) structure using the two acousto-optical deflectors D_1 and D_2 is depicted in Figure One[3]. The photo multiplier tube (PMT) using direct detection methods transmits the received intensity signals to the oscilloscope after converting them. L_3 is an integration lens. It spacially integrates the signal onto the square-law detector PMT[4]. The photocurrent output of the detector is:

In this equation, S(t) and R(t) are respectively the signal and a reference signal, D and D_2 are aperture diameters. We can see from Figure One the type of direct detection used to obtain the signal and the reference signal convolution norm. To obtain correlated output, it is necessary to perform time feedback on one of these two signals. When the signal has time axis of symmetry, the convolution and correlation are equivalent.

If S(t) and R(t) are both modulated on one linear modulation and separately entered into the two acousto-optical deflectors depicted in Figure Two, then the equipment in Figure Two can complete the Fourier transformation of signal S(t). Therefore, Illustration Two is the general structure of spacially integrated model acousto-optical Fourier transforming. However, we discovered that if we separately entered S(t) and R(t) on fixed carrier frequencies into the ultrasonic converters of the two acousto-optical deflectors in Figure Two then we could obtain the signal convolution (and not convolution norm) on a certain carrier frequency. Therefore, figure two can also be seen as a heterodyne detector space integrating acousto-optical correlation structure. Below we will derive the detector output of this structure.

The difference between Figures One and Two is the simultaneous use of the diffracted light and non diffracted light of the acousto-optical deflector to perform heterodyne detection. The frequency is ω_o, the amplitude is E_o light $E_i(=E_0\exp(i\omega t))$ at a Bragg angle of incidence D_1. The D_1 piezoelectric converter is driven by $S(t)\cos(\omega_1 t)$, (ω_1 is the carrier frequency). With appropriate adjustment of D_1 we obtain +1 level Bragg diffracted light E_1 as

$$E_1(t-\tau)=\eta_1(\omega_1)E_0S(t-\tau)\exp\{i[\omega_0 t+\omega_1(t-\tau)]\}, \qquad (2)$$

In this equation, $\tau(=z/V_s)$ (z is the coordinate along direction of acoustic transmission, V_o is ultrasonic speed) is the delay time, $\eta_1(\omega_1)$ is The diffraction efficiency (with Bragg diffraction, there is only 0 level and +1 level light) of D_1 on frequency $f_1(=\omega_1/2\pi)$.

Causing the D_1 0 level light and +1 level both pass through lenses L_1 and L_2 to D_2. Modulate D_2 so 0 level light is just at the Bragg angle to generate -1 level diffraction, and the 0 level is filtered out at the rear focal plane of L_3, and the D_1 +1 level light E_1 goes directly to D_2 without diffraction. Because of the objective relationship formed between D_1 and D_2, the $-\tau$ in D_1 will become the $+\tau$ in D_2. That is, $E_1(t-\tau) \rightarrow E_1(t+\tau)$. When the reference signal of $R(t)\cos(\omega_2 t)$ is applied to the D_2 converter (ω_2 a carrier wave) we obtain the D_2 -1 level light of diffraction

$$E_2(t-\tau) = E_0\eta_2(\omega_2)[1-\eta_1(\omega_1)]R(t-\tau)\exp\{i[\omega_0 t-\omega_2(t-\tau)]\}, \tag{3}$$

In this equation, $\eta_2(\omega_2)$ is the diffraction efficiency of at the frequency $f_2(=\omega_2^2/2\pi)$. After integration through lens L_3, $E_1(t+\tau)$ and $E_2(t-\tau)$ are focused together on the detector, and the detector outputs the photocurrent

$$I_{out} = \int_D |E_1(t+\tau)+E_2(t-\tau)|^2 d\tau = I_1+I_2+I_3, \tag{4}$$

In this equation, I_1 and I_2 are direct current items affecting the dynamic range of output. I_3 is the cross item required. Its form is

$$\left.\begin{aligned} I_3 &= K\cos[(\omega_1+\omega_2)t]\,\mathrm{Re}\left\{\int_D S(\tau)R^*(2t-\tau)\exp[i(\omega_1-\omega_2)\tau]d\tau\right\}, \\ K &= 2E_0^2\eta_1(\omega_1)\eta_2(\omega_2)[1-\eta_1(\omega_1)], \end{aligned}\right\} \tag{5}$$

In this equation, $*$ indicates the complex conjugate. When R is a real number and $\omega_1 = \omega_2$, equation (5) regresses to

$$I_3 = K\cos(2\omega_1 t)\int_D S(\tau)R(2t-\tau)d\tau, \tag{6}$$

Thus we obtain the convolution of S and R. Because this convolution is modulated on carrier frequency $2\omega_1$, it is necessary to demodulate the detector output with a low pass wave filter.

II: THE TIME INTEGRATION MODEL

Time integrated model acousto-optical correlating devices are normally composed of an acousto-optical modulator and an acousto-

optical deflector[3]. However, we can see that if suitable adjustments are made to Figure One, we can also obtain a time integration model acousto-optical correlator composed of two acousto-optical deflectors. Removing the detector from Figure One and adding lenses L_3 and L_4 to form a $4f$ system, and adding a linear array detector on the D_2 image plane will make up such an correlator. The +1 level diffracted light generated by D_1 is still shown in model 2), with the zero level light L_1 rear focal plane is filtered out. When $E_1(t-\tau)$ reaches D_2 it is changed to $E_1(t+\tau)$ (the reason for this is as explained earlier), it is projected on D_2 at Bragg angle, generating a +1 level diffraction

$$\left.\begin{aligned} E_{12}(t-\tau,\ t+\tau) &= AS(t+\tau)R(t-\tau)\exp\{i[\omega_0 t+\omega_1(t+\tau)+\omega_2(t-\tau)]\}, \\ A &= E_0\eta_1(\omega_1)\,\eta_2(\omega_2). \end{aligned}\right\} \quad (7)$$

The $\tau \to -\tau$ detector in the middle of E_{12} on the detection plane integrates the light intensity, and its output is

$$I_{out} = \int_0^T |E_{12}(t+\tau,\ t-\tau)|^2 dt = A^2 \int_0^T |S(t-2\tau)R(t)|^2 dt, \quad (8)$$

In this equation T is the integrated time of the detection array. Because T can attain microsecond levels, the time integration model acousto-optical processor has a very large time bandwidth product, thus increasing the signal noise of the output.

We can see from equation (8) that the output of this type of time integration model acousto-optical correlators with two acousto-optical reflectors are convoluted S and R norms. Furthermore, the convoluted output signal bandwidth is the algebraic average of the bandwidths of S and R. The author is of the opinion that because the detector is only capable of integration of light amplitude squares, no matter what model of time integrated correlators is used, it will only be able to obtain the convolution (correlation) of the signal norms. This is different from the conclusion reached by Sprague[3].

III: EXPERIMENTAL EQUIPMENT FOR ACOUSTO-OPTICAL SIGNALS PROCESSING

The experimental equipment was composed of an He-Ne laser, acousto-optical reflectors, simulation signal generating equipment, photoelectric detectors and number of lenses and adjustment frames. The key parts were the acousto-optical deflectors and the simulation signal generating equipment which are detailed below.

1. ACOUSTO-OPTICAL DEFECTORS

The acousto-optical deflectors used TeO_2 variable wave adjustable type elements[5]. The central frequency was 250 MHz, and the band width was greater than 100MHz. The peak diffraction efficiency was greater than 30 percent. Delay line length was 17 microseconds. For a piezoelectric converter we used $LiNbO_3$ chip. The anti-reflective film was made of Au-Ag-In-Ag.

2. SIMULATIVE SIGNAL GENERATING EQUIPMENT

The simulative signal generating equipment we designed ourselves was composed of two completely identical parts. However, the corresponding delay times signals put out by the two channels were adjustable. Figure Three presents a block diagram of half of this equipment. Its continuous signal output power could reach 1W. By choosing different switch positions, it was possible to achieve a fixed carrier frequency with a duty cycle of 0.5 or a linear frequency modulated pulse (series) output.

FIGURE THREE: SCHEMATIC OF ANALOGOUS SIGNALS GENERATOR

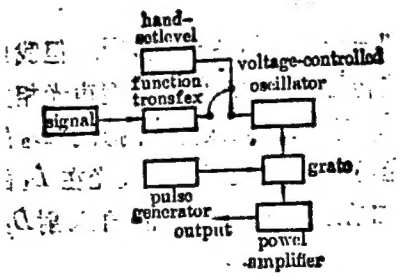

IV: EXPERIMENTAL RESULTS AND DISCUSSION

Figure Four is a photograph of the equipment used in the acousto-optical signals processing experiment. Because all the signals used in this article were rectangular pulses, it was not necessary to perform time feedback in order to obtain a correlated output.

The self correlation of N rectangular hole factors with a width of 1 and a separation of z can be written as

$$\sigma = \int \left[\sum_{n=0}^{N-1} \mathrm{rect}(\tau - 2n)\right]\left[\sum_{n=0}^{N-1} \mathrm{rect}(\tau + x - 2n)\right] d\tau, \qquad (9)$$

In this equation "rect" represents the rectangular hole factors. Each rectangular hole has a unit area. Through computation we can obtain the auto-correlation of N square hole pulses with a duty cycle of 0.5 as 2N-1 triangular pulses with the Nth triangular pulse being the axial distribution, and pulses on either side having an amplitude deviation of 1 or (2N-1) pulse amplitude. The width of each triangular pulse is twice the width of a triangular pulse. Figure Five shows the calculation result for auto-correlation of four rectangular pulses. Figure Six shows the output for the spacially integrated cross correlation of a single fixed frequency rectangular pulse. The two lines on the bottom of this illustration are two signals not yet correlated. The upper line is the correlated output (triangular pulse) modulated on a carrier wave twice the operating frequency of the acousto-optical deflector. We can see from Figure six that the width of the correlated output signal is the same as the width of the uncorrelated signals. This is because in equation (8) the (two words unknown) of R is $(2t-\tau)$. The result is the same for equations (4) and (10).

Figure Seven shows the oscilloscope display of the auto-correlation output of nine rectangular pulses on a fixed frequency radio wave obtained with direct detection. This conforms fairly

well with computed results. The reason the bases of none of the rectangular waves in Figure Seven do not come down to the zero line is that the duty cycle of the pulse string is slightly greater than 0.5 and detection runs behind. Figure Eight shows results of time integrated auto-correlation of nine rectangular pulse strings obtained through direct detection and modulated on a linear FM (LEF) carrier wave. The time integration of the 2048 position linear array CCD used can reach 10 microseconds. There are two problems with the correlation output shown in Figure Eight. The Waveform is distorted and the bases of the triangular pulses are not on the reference line. The reason for the later problem is the same for the similar problem in Figure Seven. The reason for the first problem can be found in equation (10). Because a linear modulated signal is used, $\eta_1(\omega_1)$ and $\eta_2(\omega_2)$ are no longer constants. They are weight functions added to the correlation output and they alter the waveform of the output.

It should be pointed out that the acousto-optical correlation structure pictured in Figure Two is fully capable of Fourier transformation of signals. However it requires the mixing of the signals and one baseband linear modulated frequency before it is entered into the acousto-optical modulator. The signal conversion output is modulated on a linear modulated signal four times the base band. The problems with this type of processing with the demodulation of the signals. A similar demodulation technology has been reported[6], which can separately obtain real and imaginary portions of the Fourier Spectrum.

FIG. 4: EXPERIMENTAL SYSTEM FOR ACUSTO-OPTICAL SIGNAL PROCESSING

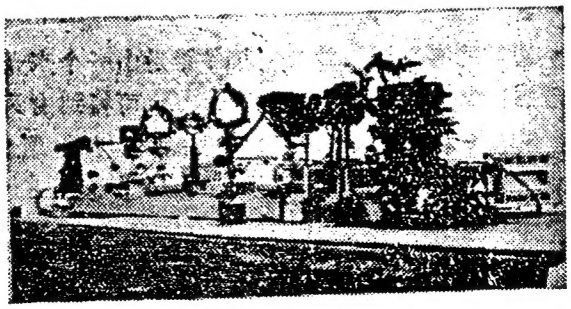

Fig. 5 Calculating result of auto-correlation for four rect pulses

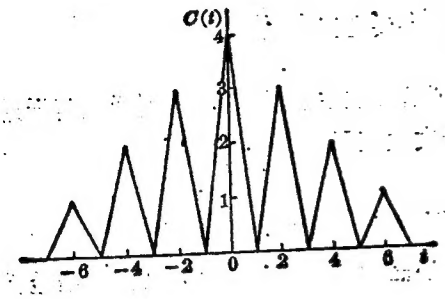

Fig. 6 Cross correlation of single rect pulse using heterodyne detection. Horizontal scale is in units of 1 μs/cm. (SI)

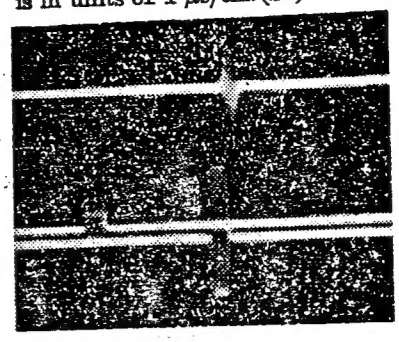

Fig. 7 Auto-correlation output of nine rect pulses obtained with direct detection Horizontal scale is in units of 2 μs/cm. (SI)

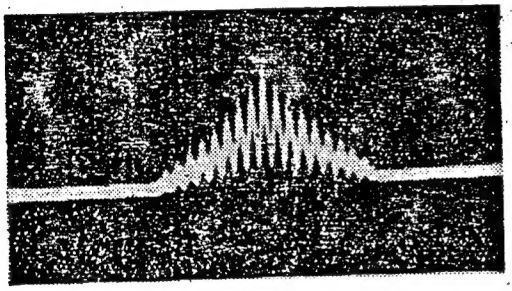

Fig. 8 TI auto-correlation output of nine rect pulses modulated on LFM obtained with direct detection

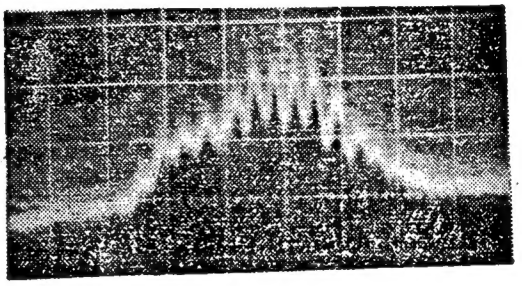

V: CONCLUSIONS

The characteristics of acousto-optics, a new signals processing technology, are presented through experiments in this article. Although our results of spacial integration and time integration acousto-optical convolution (correlation) experiments on a number of simulative signals using direction detection and heterodyne detection methods are preliminary, they are fairy satisfying. The addition of the heterodyne detection method helps increase the signal to noise ratio of the output. Because we used

a new model high frequency wideband acousto-optical device, it greatly increased the spacial (time) bandwidth product of the system, increasing processing gain. This advantage is even more prominent when using time integrated models. Further improvements of the experimental system to improve acousto-optical signals processing capabilities (such as Fourier conversion) would undoubtedly be of significance and we will work toward this in the future.

Finally, the author would like to show his appreciation to comrade Liang Yuexi of the Xianke Laser and Television Company of Shenchuan for the encouragement received through our wide-ranging discussions, to comrade Wang Fuyuan of the Academy of Sciences Institute of Optics and Electronics for his helpful technological guidance in my experiments and to comrades Xu Jiaren, Yang Shulan and Zhang Chunhua for making the Acousto-optical devices used in this experiment.

VI: BIBLIOGRAPHY

[1] L. N. Florses, D. L. Hetch; *Proc. SPIE*, 1977, **118**, 182~192.
[2] D. Psaltis; *Opt. Engng*, 1980, **19**, No. 2 (Mar-Apr), 193~199.
[3] R. A. Sprague; *Opt. Engng*, 1977, **16**, No. 5 (Sep-Oct), 467~474.
[4] A. Korpel; «*Optical Information Processing*», (Plenum Press, New York, 1976), 171~175.
[5] 李宁;«中国激光», 1986, **13**, No. 8 (Aug), 493~497.
[6] D. F. Hotz; *Appl. Opt.*, 1984, **23**, No. 10 (May), 1613~1619.

[5]. Li Ning; "China Lasers", 1986, 13, no.8 (Aug), 498-497.

DISTRIBUTION LIST

DISTRIBUTION DIRECT TO RECIPIENT

ORGANIZATION	MICROFICHE
B085 DIA/RTS-2FI	1
C509 BALLOC509 BALLISTIC RES LAB	1
C510 R&T LABS/AVEADCOM	1
C513 ARRADCOM	1
C535 AVRADCOM/TSARCOM	1
C539 TRASANA	1
Q592 FSTC	4
Q619 MSIC REDSTONE	1
Q008 NTIC	1
Q043 AFMIC-IS	1
E051 HQ USAF/INET	1
E404 AEDC/DOF	1
E408 AFWL	1
E410 AFDTC/IN	1
E429 SD/IND	1
P005 DOE/ISA/DDI	1
P050 CIA/OCR/ADD/SD	2
1051 AFIT/LDE	1
P090 NSA/CDB	1
2206 FSL	1

Microfiche Nbr: FTD94C000474L
NAIC-ID(RS)T-0369-94